AIP Journal of Applied Physics

Reassessment of the recombination parameters of chromium in n- and p-type crystalline silicon and chromium-boron pairs in p-type crystalline silicon

Chang Sun, Fiacre E. Rougieux, and Daniel Macdonald

Citation: Journal of Applied Physics **115**, 214907 (2014); doi: 10.1063/1.4881497
View online: http://dx.doi.org/10.1063/1.4881497
View Table of Contents: http://scitation.aip.org/content/aip/journal/jap/115/21?ver=pdfcov
Published by the AIP Publishing

Articles you may be interested in

Impact of oxygen on the permanent deactivation of boron–oxygen-related recombination centers in crystalline silicon
J. Appl. Phys. **107**, 123707 (2010); 10.1063/1.3431359

Recombination activity of interstitial chromium and chromium-boron pairs in silicon
J. Appl. Phys. **102**, 123701 (2007); 10.1063/1.2822452

Determination at 300 K of the hole capture cross section of chromium-boron pairs in p -type silicon
Appl. Phys. Lett. **89**, 232112 (2006); 10.1063/1.2402261

Doping dependence of the carrier lifetime crossover point upon dissociation of iron-boron pairs in crystalline silicon
Appl. Phys. Lett. **89**, 142107 (2006); 10.1063/1.2358126

Electronic properties of light-induced recombination centers in boron-doped Czochralski silicon
J. Appl. Phys. **86**, 3175 (1999); 10.1063/1.371186

is pleased to announce Reuben Collins
as its new Editor-in-Chief

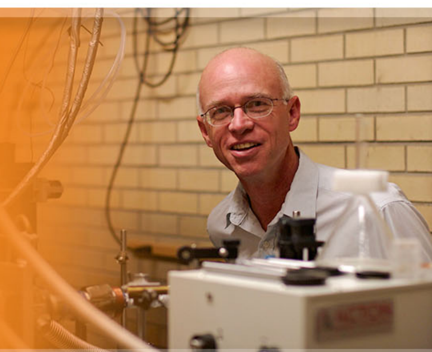

[This article is copyrighted as indicated in the article. Reuse of AIP content is subject to the terms at: http://scitation.aip.org/termsconditions. Downloaded to] IP: 130.56.107.193 On: Mon, 15 Sep 2014 05:43:37

JOURNAL OF APPLIED PHYSICS 115, 214907 (2014)

Reassessment of the recombination parameters of chromium in n- and p-type crystalline silicon and chromium-boron pairs in p-type crystalline silicon

Chang Sun,[a] Fiacre E. Rougieux, and Daniel Macdonald
Research School of Engineering, College of Engineering and Computer Science, The Australian National University, Canberra ACT 0200, Australia

(Received 3 April 2014; accepted 22 May 2014; published online 3 June 2014)

Injection-dependent lifetime spectroscopy of both n- and p-type, Cr-doped silicon wafers with different doping levels is used to determine the defect parameters of Cr_i and CrB pairs, by simultaneously fitting the measured lifetimes with the Shockley-Read-Hall model. A combined analysis of the two defects with the lifetime data measured on both n- and p-type samples enables a significant tightening of the uncertainty ranges of the parameters. The capture cross section ratios $k = \sigma_n/\sigma_p$ of Cr_i and CrB are determined as 3.2 (−0.6, +0) and 5.8 (−3.4, +0.6), respectively. Courtesy of a direct experimental comparison of the recombination activity of chromium in n- and p-type silicon, and as also suggested by modelling results, we conclude that chromium has a greater negative impact on carrier lifetimes in p-type silicon than n-type silicon with similar doping levels. © *2014 AIP Publishing LLC*. [http://dx.doi.org/10.1063/1.4881497]

I. INTRODUCTION

Transition-metal impurities, such as chromium, are detrimental to silicon devices. Both dissolved and precipitated transition metals can cause increased recombination activity and reduce the carrier lifetime,[1] yet such impurities are common in photovoltaic grade crystalline silicon materials.[2] Chromium is a common contaminant, and previous studies have shown its concentration of chromium in photovoltaic-grade multicrystalline silicon wafers can be in the 10^{12}–10^{13} cm^{-3} range.[2,3]

In n-type silicon (n-Si), dissolved chromium only exists as isolated interstitial chromium (Cr_i), forming a donor level; while in p-Si, the donor level of Cr_i is positively charged at room temperature and will form donor-acceptor pairs with the negatively charged acceptor level of the doping element, such as boron (CrB pairs).[1] This is analogous to the case of Fe, which can exist as isolated Fe_i or FeB pairs in p-Si.[1] However, while illumination or injection of minority carriers can break the FeB pairs, several authors have shown that such electronically stimulated dissociation does not apply to CrB pairs.[4,5] As it has been shown that such donor-acceptor pairs are formed only when Coulombic attraction is present between the oppositely charged ions,[6,7] the illumination-related phenomenon can be explained by the different energy level of Fe_i and Cr_i: the electron Fermi level is shifted above the energy level of Fe_i under illumination, leaving this donor in a neutral charge state, which will prohibit re-pairing during illumination; yet it is almost impossible to shift the electron Fermi level above the Cr_i level, as it is much closer to the conduction band, meaning that CrB pairs can reform rapidly during illumination.[6,8]

The different recombination properties of the paired and dissociated states in p-Si allows a method originally developed to determine the concentration of Fe,[9,10] to be applied to determine the Cr concentration.[4,5,11] More recently, it has been shown that the use of photoluminescence-based carrier lifetime images[12] allows the same principle to be used to determine the spatial distributions of Fe,[13] Cr,[14] and boron-oxygen (BO) complex.[15,16] Being fast and contactless, these techniques can conveniently provide information about the concentration and distribution of impurities. Nevertheless, for these new techniques to be accurate, it is vital to have a precise determination of the defect recombination parameters—namely, the energy level and the capture cross sections for both electrons and holes.

Courtesy of Deep-Level Transient Spectroscopy (DLTS) and Lifetime Spectroscopy, there are well-established values for the energy levels of Cr_i and CrB pairs: Cr_i produces a single donor level at $E_c - 0.22(\pm 0.02)$ eV and CrB pairs produce a donor level at $E_v + 0.28(\pm 0.02)$ eV.[1,4,5,17] However, the published values of the capture cross sections for electrons and holes are less consistent and vary across orders of magnitudes. Another important parameter, the capture cross section ratio $k = \sigma_n/\sigma_p$, also varies significantly in published works and is often not reported as DLTS generally does not permit both cross sections to be measured.[1] However, k is an important parameter as it determines the relative impact of an impurity in n- and p-type silicon at low and mid-injection levels. Such a comparison of the recombination activity in n- and p-Si has been studied directly for metals such as iron,[18] nickel,[19] and copper,[20] but not so thoroughly for chromium.

Injection-Dependent Lifetime Spectroscopy (IDLS) offers a convenient method to determine the defect parameters, by fitting the injection-dependent lifetime with the Shockley-Read-Hall (SRH) model. To allow unambiguous measurement of the defect parameters, a sample can also be measured at different temperatures, a method termed Temperature- and Injection-Dependent Lifetime Spectroscopy (TIDLS).[21] An alternative method is to simultaneously fit the

[a]Electronic mail: chang.sun@anu.edu.au.

 © 2014 AIP Publishing LLC

[This article is copyrighted as indicated in the article. Reuse of AIP content is subject to the terms at: http://scitation.aip.org/termsconditions. Downloaded to] IP: 130.56.107.193 On: Mon, 15 Sep 2014 05:43:37

injection-dependent lifetime measured on several samples with different doping levels.[22,23] In this work, we use this latter method to determine the defect parameters with several n- and p-type samples. We will also provide the uncertainties associated with the recombination parameters. Crucially, the simultaneous use of both n- and p-type samples allows the capture cross sections to be determined with significantly reduced uncertainty. The results also allow a direct experimental comparison of the recombination activity of chromium in both n- and p-type silicon.

II. EXPERIMENTAL METHODS

A. Sample preparation

The samples used in this study were from four Czochralski (Cz) ingots specially grown by Siliconsultant.[24] One p- and n-type ingots were grown as control ingots, and one p- and n-type ingots were intentionally doped with chromium. The 25 mm diameter ingots (average) were then cut to wafers. 3–5 wafers selected at different solidified fractions were then chosen for this study. When preparing the ingots, the targeted dopant and impurity concentration calculations were performed based on Scheil's law[25,26]

$$C = k_{eff} \cdot C_0 (1-g)^{k_{eff}-1}, \tag{1}$$

where C_0 is the concentration in starting melt, k_{eff} is the effective segregation coefficient, and g is solidified fraction. The n-type ingots were doped with phosphorus and the p-type ingots with boron. At $g = 0.3$, the target doping concentration was $1.5 \times 10^{16}\,\mathrm{cm^{-3}}$. We also measured the doping levels of the samples by dark conductance measurements. Figure 1 shows the doping levels of two Cr-doped ingots and the fits using Scheil's law (Eq. (1)), with k_{eff} of boron and phosphorous taken as 0.8 and 0.35,[27] respectively. The relative error is taken as 5%,[28] shown with the error bars. The deviation of the actual doping levels from the target values is due to the uncertainty in the mass of the dopants in the starting melt. As determined by a Fourier Transform Infrared (FT-IR) spectrophotometer, the lower limit of the concentration of interstitial oxygen [O_i] in our samples is around $6 \times 10^{17}\,\mathrm{cm^{-3}}$. With the effective segregation coefficient of Cr taken as 1.1×10^{-5},[29,30] and targeting a Cr concentration of about $1 \times 10^{12}\,\mathrm{cm^{-3}}$ in the ingots, C_0 for chromium was chosen as $4.8 \times 10^{16}\,\mathrm{cm^{-3}}$, requiring 0.0009 g of chromium in the starting melt. In order to minimize surface recombination, the wafers were silicon-etched and then passivated with Plasma-Enhanced Chemical Vapor Deposited (PECVD) SiN films. This technique provides very low surface recombination velocities.[31,32] Moreover, the SiN passivation is shown to be stable after the thermal treatments required for dissociation and association of CrB pairs.

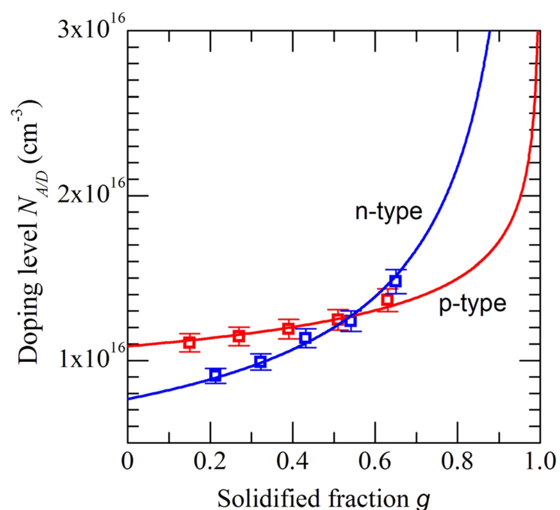

FIG. 1. Measured doping levels of the Cr-doped ingots, fitted to Scheil's law.

B. Dissociation and association of CrB pairs

Measuring the lifetime for the case of isolated Cr_i in p-type silicon requires the CrB pairs to first be broken. The dissociation of CrB pairs is driven by annealing, where the fraction of isolated Cr_i in thermal equilibrium is given by[17]

$$\frac{\mathrm{CrB}}{\mathrm{Cr_i}} = \frac{N_A}{A} \times \exp\left(\frac{E_A}{k_B T}\right), \tag{2}$$

with A being the density of available interstitial sites. Conzelmann *et al.* initially determined a binding energy of $E_A = 0.65\,\mathrm{eV}$ with $A = 8 \times 10^{23}\,\mathrm{cm^{-3}}$,[17] values which were later determined more precisely by Habenicht *et al.* as $E_A = 0.56\,\mathrm{eV}$, with $A = 5 \times 10^{22}\,\mathrm{cm^{-3}}$.[14] We used the coefficient derived by Habenicht *et al.* to predict the fraction of isolated Cr_i in thermal equilibrium at several temperatures, shown in Table I. As shown, temperatures above 230 °C are required to ensure 90% or more of the CrB pairs are broken. In the work of Schmidt *et al.* for samples of resistivity 11.4 Ω·cm, the dissociation time constant τ_{diss} was found to be 48 s at 160 °C.[5] At higher temperatures, the kinetics of the dissociation speeds up. To achieve a state where there is a high fraction of isolated Cr_i, the p-type samples were annealed in this work at around 260 °C in the dark for 8 min and subsequently quenched in water. This annealing step also effectively deactivates the BO complex,[33] while the quenching avoids repairing of CrB pairs during cooling down.

To measure the association kinetics of CrB pairs, less strict conditions are required, where we annealed the p-type samples at 230 °C–250 °C in the dark for at least 5 min and cooled them down on an aluminium block. It takes several seconds for the samples to reach room temperature. Upon

TABLE I. Fraction of isolated Cr_i and the association time constant τ_{assoc} at different temperatures, predicted with data from the works of Habenicht *et al.* and Nakashima *et al.* An average doping level of $N_A = 1.2 \times 10^{16}\,\mathrm{cm^{-3}}$ for p-type samples is used in the calculations.

T (°C)	Fraction of isolated Cr_i (%)	τ_{assoc} (s)
270	96	0.8
250	94	1.6
230	90	3.2
200	78	9.5

[This article is copyrighted as indicated in the article. Reuse of AIP content is subject to the terms at: http://scitation.aip.org/termsconditions. Downloaded to] IP: 130.56.107.193 On: Mon, 15 Sep 2014 05:43:37

reaching room temperature, the samples are immediately measured. The samples are then measured after different lengths of time (0.5 h, 2 h, 4 h, 7 h, and 10 h), while holding them at 53 °C in between the measurements. The measurements are performed at room temperature. This kinetics can be described by[34]

$$\frac{\mathrm{CrB}}{\mathrm{Cr_i}} = 1 - \exp\left(-\frac{t}{\tau_{assoc}}\right), \tag{3}$$

τ_{assoc} being the association time constant. In units of seconds, τ_{assoc} is related to the diffusivity of interstitial chromium D_{Cr_i} and the doping level N_A by[35]

$$\tau_{assoc} = \frac{557T}{N_A D_{\mathrm{Cr_i}}}. \tag{4}$$

Nakashima *et al*. determined D_{Cr_i} in the temperature range of 27 °C–400 °C.[36] From their data, the highest τ_{assoc} is predicted to be 11 h for all the p-type Cr-doped samples at 53 °C, a temperature where the dissociation process can be completely neglected. However, as found by several other authors[5,11] as well as this study, the diffusivity data found by Nakashima *et al*. tend to be a little lower and will thus generate higher time constants. Accordingly, we kept the samples at about 53 °C in the dark for 4 days to confidently produce the fully associated state.

C. Lifetime measurements

The injection-dependent lifetime measurements were performed using the Quasi-Steady State PhotoConductance method (QSSPC).[37] Note that as our samples are smaller than the standard sensor region, we used a modified calibration procedure to account for the different sample geometry.[38] Also as the Cr-doped samples have thicknesses around 450 μm and relatively low lifetimes, an infrared filter was used to achieve more uniform generation profiles, and thus more uniform carrier profiles across the wafer depth.

Iron-boron (FeB) pairs and the BO complex are two other well-known metastable defects which may impact on lifetime measurements in p-type Cz silicon.[15] With the p-type Cr-doped samples in the fully associated state, we compared the lifetime curves measured before and after illuminating them with a strong white flash, finding no significant change. This ensures that no serious iron contamination is present in our samples, as FeB pairs are expected to be dissociated by the optical illumination, which would lead to a detectible change in the carrier lifetime curves.[10]

As discussed before, the concentration of interstitial oxygen [O_i] in our samples is more than $6 \times 10^{17}\,\mathrm{cm^{-3}}$. This will result in a non-negligible amount of BO complexes.[33] This defect can be deactivated at temperatures around 200 °C, and reactivated by optical illumination.[33,39] With a 1.1 Ω·cm p-type Cz-Si sample, which has a similar doping level as the p-type samples studied in this work, Schmidt *et al*. found a defect annihilation time constant of about 20 s at 200 °C.[33] This result gives us confidence that the procedure we used to break CrB pairs (>230 °C, 5 min) also enables complete deactivation of the BO complex. To avoid re-activation of the BO defect, the samples are always kept in the dark, except when the measurements were performed. When repeated measurements are performed on control samples, a slight degradation of lifetime was observed, which is likely caused by some activation of the BO complex. However, the lowest lifetime of the control samples was always more than one order of magnitude higher than the Cr-doped samples over the whole injection range measured. Hence, we can safely assume that the influence of the BO complex is negligible in our analysis.

Figure 2 shows the injection-dependent lifetime curves of the Cr-doped p- and n-type samples, together with the corresponding control samples. As shown by the comparison, the lifetime of the control samples is always one to two orders of magnitude higher than that of the Cr-doped samples. This ensures that the lifetime of the Cr-doped samples is dominated by bulk SRH recombination caused by Cr-related centers.

III. MODELLING PROCEDURE

In this work, we attempt to determine the defect parameters of $\mathrm{Cr_i}$ and CrB pairs by measuring the injection-dependent lifetime data and fitting by a simplified model for SRH statistics.[40,41] This simplification is valid for a defect density significantly lower than the doping, which is valid in our samples. The SRH lifetime in n-Si is given by[40,41]

$$\tau_{SRH} = \frac{k(N_D + n_1) + (k+1)\Delta n + p_1}{N_t \sigma_n v_{th}(N_D + \Delta n)}, \tag{5}$$

and for p-Si

$$\tau_{SRH} = \frac{N_A + (k+1)\Delta n + p_1 + kn_1}{N_t \sigma_n v_{th}(N_A + \Delta n)}, \tag{6}$$

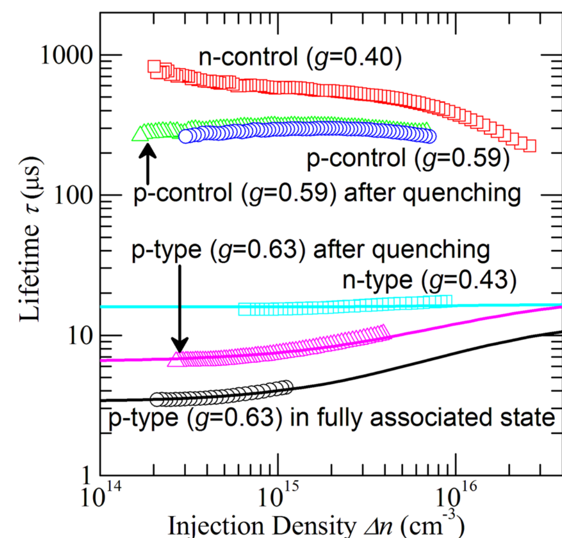

FIG. 2. Lifetime measurements for samples n-type ($g = 0.43$), p-type ($g = 0.63$), and corresponding control samples. For the p-type samples, measurements performed both directly after quenching and in the fully associated state are shown. The data are fitted with the defect parameters found in this work (Table II).

[This article is copyrighted as indicated in the article. Reuse of AIP content is subject to the terms at: http://scitation.aip.org/termsconditions. Downloaded to] IP: 130.56.107.193 On: Mon, 15 Sep 2014 05:43:37

n_1 and p_1 being the equilibrium electron and hole densities when the defect energy level coincides with the Fermi level, σ_n being the electron capture cross section, k being the capture cross section ratio σ_n/σ_p, and N_t being the density of the defect. The thermal velocity v_{th} is taken as 1.1×10^7 cm^2/s.[42] For both types, the defect energy which determines n_1 and p_1, the capture cross section ratio k and the product of $N_t\sigma_n$ can be viewed as the only three parameters to be determined by fitting this model. In this work, we will determine fitted values of $N_t\sigma_n$ for all the samples, fit them to Scheil's law (Eq. (1)) and obtain a value for $\sigma_n C_0$. By using an estimated value of the concentration of chromium in the starting melt C_0, we are then able to estimate the electron capture cross section. The hole capture cross section is then estimated via the capture cross section ratio.

A common method used in data fitting is the least squares method, where the optimal parameters are found to minimize the sum of squared residuals, S. If we make allowance for the uncertainties in the lifetime data, the model generates a feasible zone, where the combinations of the parameters enable the lifetime predicted by the model to be within the relative error of e_r when compared with the experimental data. Blum *et al.* investigated the inter-laboratory repeatability of the lifetime measured with QSSPC, reporting this relative error e_r to be about 11% for the quasi-steady-state mode.[28]

With three parameters to be determined, we vary the values of two parameters, allowing for an optimal value of the third parameter to be determined, then calculate S at every point and observe where the "least squares" occurs. When applied to the lifetime data measured on n-type samples to determine the defect parameters of Cr_i, a very large range of the capture cross section ratio k is given first (0–500), and for each value of k in this range, the energy level E_t is varied throughout the whole band gap, generating different optimal values of $N_t\sigma_n$ in the fitting. Corresponding to each combination of the parameters, the residual at each lifetime data point can be calculated. Then, we obtain the optimal values of the parameters with the least squares method and also obtain their ranges by making allowance for uncertainties in the lifetime data.

In the p-type samples, the SRH lifetime was found to be much less sensitive to variations in the energy level of CrB pairs, the likely cause being the smaller range of doping levels of the p-type samples. The curves in Figure 1 outline the smaller dopant variation expected for p-type (boron-doped) ingots, resulting in a smaller range of N_A we could achieve in the p-type samples. This in turn makes it impossible to obtain a well-defined energy level from the fitting. However, as the energy level of CrB pairs published in the literature is in fact, in a very small range, we have therefore chosen to fix the energy level within this small range when fitting the SRH lifetime of CrB pairs.

The third set of lifetime data, those measured on p-type samples directly after quenching in water were found to play an important role in the accurate determination of the defect parameters in this study. In this state, there is a high fraction of isolated Cr_i, with the remaining dissolved chromium existing as CrB pairs. Therefore, the defect parameters of both Cr_i as well as CrB pairs are involved in the fitting. As we have already determined the ranges of k^{Cr_i} with the n-type samples and k^{CrB} with p-type samples in the fully associated state, we input these ranges into the model first. For every value of k^{Cr_i}, there is an optimal value for $\sigma_n C_0$ for Cr_i determined by the lifetime data of n-type samples. And for every value of k^{CrB}, there is an optimal value for $\sigma_n C_0$ for CrB pairs as well as a group of $N_t\sigma_n$ determined by the lifetime data of CrB pairs. According to the procedures used in the preparation of the ingots, we estimate C_0 to be in the range of 2.7×10^{16} cm^{-3}–7.5×10^{16} cm^{-3}. In the procedure of determining the optimal combinations of all those parameters or a feasible zone with the third set of lifetime data, at the same time of varying the values of the two capture cross section ratios, we also vary the values of C_0 for the n-type samples and p-type samples, separately, as C_0 may not be the same for both ingots. At every point, where both k and both C_0 are determined, both electron capture cross sections for Cr_i and CrB pairs can be determined. Also determined are the chromium concentrations in the p-type samples. Then the only free parameter left is the fraction of isolated Cr_i. We can estimate this fraction using data listed in Table I. As predicted, more than 90% CrB pairs are expected to be dissociated above 230 °C, but at temperatures of 200 °C–230 °C, some interstitial chromium could repair with boron in seconds, reducing the fraction to less than 80%. As the samples were quenched in water directly from high temperatures around 260 °C, we estimate the fraction of isolated Cr_i in all the five samples to be above 85%. With the ranges of all the parameters fixed, we can then fit the lifetime data and obtain the optimal values. Most importantly, this procedure enables a significant tightening of the feasible ranges, where the combinations of the parameters enable the model to fit well with all three sets of lifetime data.

IV. RESULTS AND DISCUSSION

A. Association kinetics in p-type Cr-doped samples

Figure 3 depicts the injection-dependent lifetime of a p-type Cr-doped sample measured as a function of time when kept at 53 °C, after a dissociation anneal at above 230 °C. A reduction in the lifetime was observed over the whole injection range. The same measurements were performed on all other p-type Cr-doped samples as well as the p-type control samples, the lifetimes of which were observed to be always one to two orders of magnitude higher than those of the Cr-doped samples.

The inverse lifetimes at injection level of $\Delta n = 1 \times 10^{15}$ cm^{-3} are then used to fit the CrB pairs association kinetics

$$\frac{1}{\tau} = A\exp\left(-\frac{t + t_0}{\tau_{assoc}}\right) + B, \tag{7}$$

as shown in Figure 4, and generate the association time constant τ_{assoc}. The fitted values of τ_{assoc} are around 5 h, mostly with lower values for samples with higher doping levels, which is in agreement with Eq. (4). With Eq. (4), an average diffusivity $D_{Cr_i} = 8.02 \times 10^{-16}$cm^2/s is obtained for 53 °C.

[This article is copyrighted as indicated in the article. Reuse of AIP content is subject to the terms at: http://scitation.aip.org/termsconditions. Downloaded to] IP: 130.56.107.193 On: Mon, 15 Sep 2014 05:43:37

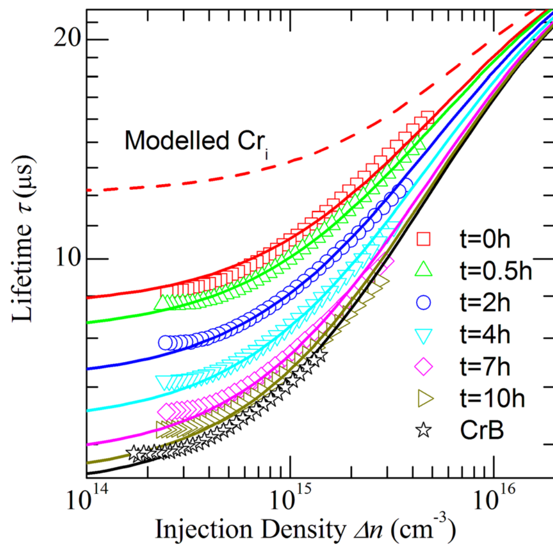

FIG. 3. Injection-dependent lifetime of sample p-type ($g = 0.39$) measured as a function of time when kept at 53 °C after annealing. Lifetime measured at the fully associated state is also shown (τ_{CrB}). The data are fitted (solid line) with the defect parameters found in this work (Table II), which are also used to model the SRH lifetime where CrB pairs are fully dissociated (τ_{Cr_i}, shown as the dashed line).

This value is in reasonable agreement with 4.16×10^{-16} cm^2/s predicted by the data of Nakashima *et al.*,[36] which, as previously mentioned, tend to give lower diffusivity values. For comparison, Fe has a diffusivity of 6.88×10^{-14} cm^2/s at this temperature,[36] two orders of magnitude higher than chromium. This further confirms that the observed degradation of lifetime is caused by the transformation of Cr$_i$ into CrB pairs.

B. Defect parameters of Cr$_i$

Figure 5 shows the lifetime measurements for the n-type Cr-doped samples. This set of lifetime data are fitted with the method described in Sec. III. Figure 6(a) shows a scan of the sum of squared residuals S when the energy level is varied throughout the band gap, with the capture cross section

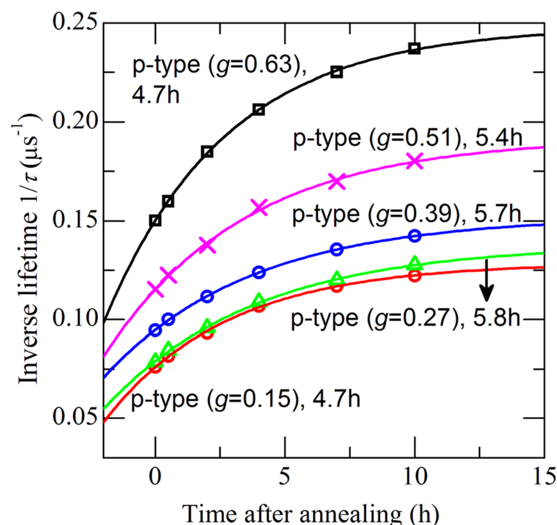

FIG. 4. Inverse lifetime at $\Delta n = 1 \times 10^{15}$ cm^{-3} as a function of time after annealing for the five p-type Cr-doped samples. The data are used to fit Eq. (4) to generate the association time constant τ_{assoc}, as shown for each curve.

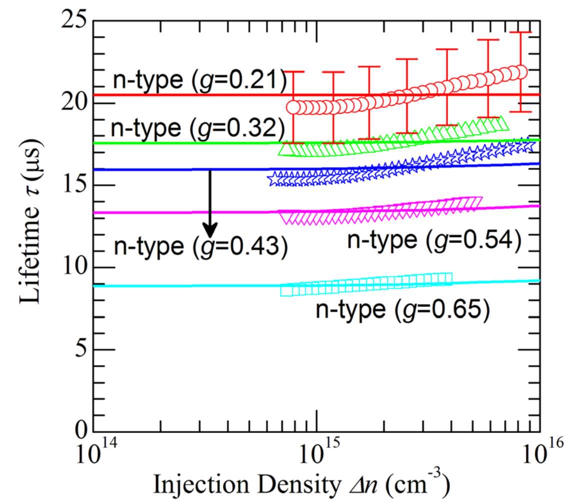

FIG. 5. Lifetime measurements (symbols) and SRH fits (solid lines) for n-type Cr-doped samples. The data are fitted (solid line) with the defect parameters found in this work (Table II). The 11% relative error is shown for sample n-type ($g = 0.21$).

ratio k^{Cr_i} fixed at its optimal value of 1.4 determined through fitting this set of lifetime data. The curves show a minimum in the upper half of the band gap and another in the lower half. As the minimum in the upper half of the band gap is the global minimum, we identify E_c-$E_t = 0.24$ eV as the most likely energy level for Cr$_i$, which is in good agreement with the literature (Table II). Figure 6(b) shows S as a function of k^{Cr_i} when E_c-$E_t = 0.24$ eV. Only one minimum at $k^{Cr_i} = 1.4$ was observed on this curve, even when the upper limit of the given range is extended to be as large as 500. By doing this, we achieve a high degree of certainty that the optimal value of k^{Cr_i} fitted by this set of lifetime data is indeed around 1.4.

A plot of the optimal values of $N_t\sigma_n$ in the five n-type samples, as a function of solidified fraction, is shown in Figure 7, fitted to Scheil's law (Eq. (1)). A value of $\sigma_n C_0$ is generated by the fitting.

Allowing 11% relative error in the lifetime data, the fitting generates a range of (0.7, 12.8) for k^{Cr_i}, a quite high upper limit. However, as can be seen in Figure 5, all of the measured curves present a slight but definite increasing trend, which is very likely a real effect, despite being smaller than the 11% relative error assumed. We may use this observed trend to reduce the uncertain range in the k factor. For n-Si with a SRH lifetime given by Eq. (5), we have

$$\frac{\partial \tau_{SRH}}{\partial \Delta n} = \frac{1}{\sigma_n v_{th} N_t (N_D + \Delta n)^2} \times (N_D - p_1 - k n_1), \quad (8)$$

from which we know that the trend of lifetime curves mainly depends on the sign of $(N_D - p_1 - kn_1)$. As we experimentally measure an increase of the lifetime as a function of injection this means that $k < (N_D - p_1)/n_1$. Using the previously determined energy level and the doping levels of our n-type samples, this bound gives an upper limit on k^{Cr_i} of about 3.2.

Schmidt *et al.* have conducted experiments on a single n-type sample with $N_D = 1.74 \times 10^{15}$ cm^{-3}, where a slightly decreasing trend of the injection-dependent lifetime curve at

[This article is copyrighted as indicated in the article. Reuse of AIP content is subject to the terms at: http://scitation.aip.org/termsconditions. Downloaded to] IP: 130.56.107.193 On: Mon, 15 Sep 2014 05:43:37

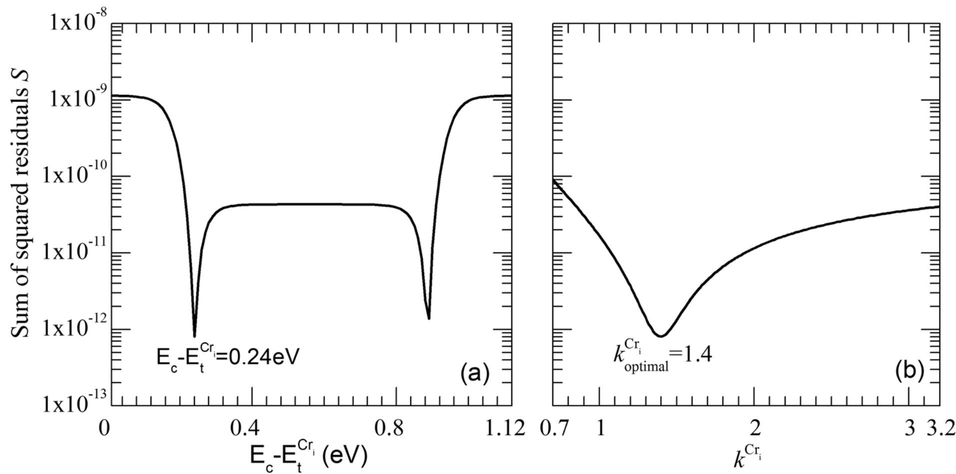

FIG. 6. (a) The sum of squared residuals S as a function of $(E_c - E_t^{Cr_i})$ when k^{Cr_i} is fixed as 1.4, which is the optimal value generated by fitting the lifetime data of n-type samples. The optimal value of $E_c - E_t^{Cr_i}$ is 0.24 eV. (b) S as a function of k^{Cr_i} when $E_c - E_t^{Cr_i} = 0.24$eV, with an optimal value of 1.4, and a range of (0.7, 3.2). The energy level and the capture cross section ratio are fitted at the same time.

TABLE II. Defect parameter of Cr_i and CrB pairs found in this work, in comparison with literature.

Cr_i	$E_c - E_t$ (eV)	σ_n (cm^2)	σ_p (cm^2)	k	Reference
Conzelmann	0.23	20×10^{-14}			17
Hangleiter			0.91×10^{-14}		43
Nakashima	0.22	1.4×10^{-14}			36
Mishra	0.22	25×10^{-14}	12.5×10^{-14}	2	4
Graff	0.22	0.73×10^{-14}			1
Schmidt	0.24	2×10^{-14}	0.4×10^{-14}	5	5
Habenicht	0.24	2×10^{-14}	0.4×10^{-14}	5	14
This work	0.24	$2.4\ (-1.0, +0.3) \times 10^{-14}$	$0.8\ (-0.3, +0.2) \times 10^{-14}$	3.2 (−0.6, +0)	
CrB	$E_t - E_v$ (eV)	σ_n (cm^2)	σ_p (cm^2)	k	Reference
Conzelmann	0.27		1×10^{-14}		17
Hangleiter		5.45×10^{-14}	1.82×10^{-14}	3	43
Nakashima	0.29		0.21×10^{-14}		36
Mishra	0.27	15×10^{-14}	0.25×10^{-14}	60	4
Graff	0.28		0.15×10^{-14}		1
Dubois			8.4×10^{-14}		11
Schmidt	0.28	0.5×10^{-14}	1×10^{-14}	0.5	5
Habenicht	0.27	2×10^{-14}	1×10^{-14}	2	14
This work	0.27	$3.8\ (-1.6, +0.5) \times 10^{-14}$	$0.7\ (-0.3, +0.6) \times 10^{-14}$	5.8 (−3.4, +0.6)	

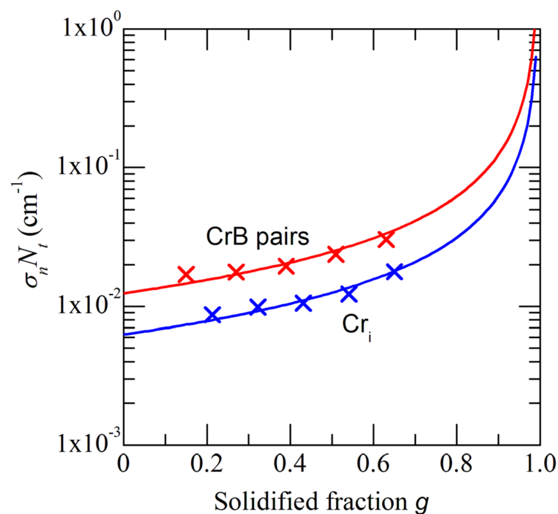

FIG. 7. The product of the electron capture cross section σ_n and the concentration of defect N_t (Cr_i or CrB pairs) as a function of solidified fraction g, fitted to Scheil's law.

room temperature was observed.[5] We may check if the range of k^{Cr_i} determined here is consistent with their finding. With the energy level of $E_c - E_t = 0.24$ eV found by both works, we have $N_D - p_1 - kn_1 = (1.74 - 2.80\,k^{Cr_i}) \times 10^{15}\text{cm}^{-3}$. With k^{Cr_i} in the range of (0.7, 3.2), this quantity is always negative, and thus a decreasing trend is indeed expected in the lifetime curve, which is consistent with their result.

C. Defect parameters of CrB pairs

Figure 8 shows the lifetime measurements for the p-type Cr-doped samples in the fully associated state. All the curves present a more pronounced injection level dependence than the n-type samples. The energy level of CrB pairs was found to be $E_t - E_v = 0.27$ eV by fitting this set of data.

Figure 9 shows the sum of squared residuals S as a function of the capture cross section ratio of CrB pairs, k^{CrB}, when the energy level is fixed at its optimal value. The minimum S is observed at $k^{CrB} = 4.6$. Similar to the n-type samples, we then generate a group of $N_t\sigma_n$ values and fit them to

[This article is copyrighted as indicated in the article. Reuse of AIP content is subject to the terms at: http://scitation.aip.org/termsconditions. Downloaded to] IP: 130.56.107.193 On: Mon, 15 Sep 2014 05:43:37

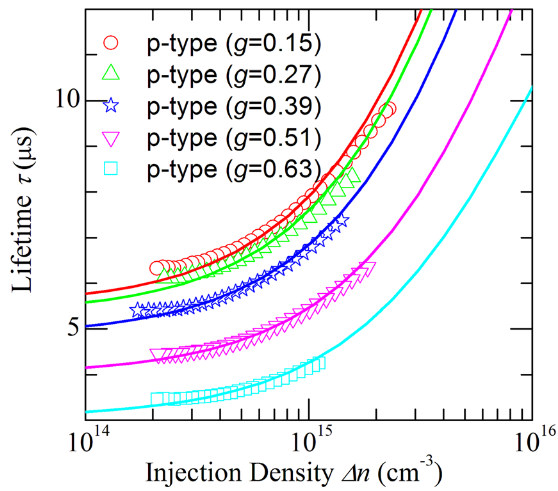

FIG. 8. Lifetime measurements (symbols) and SRH fits (solid lines) for p-type Cr-doped samples in the fully associated state. Defect parameters found in this work (Table II) are used in the fitting.

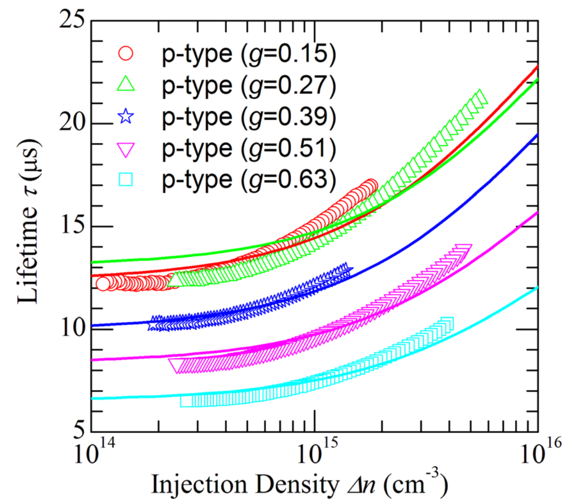

FIG. 10. Lifetime measurements (symbols) and SRH fits (solid lines) for p-type Cr-doped samples directly after quenching. Defect parameters found in this work (Table II) are used in the fitting.

Scheil's law (Eq. (1)), as shown in Figure 7. Allowing a relative error of 11%, the range of k^{CrB} is determined as (2.3, 6.8). Note that the range of capture cross section ratio is significantly narrower for CrB pairs in the p-type samples when compared to Cr_i in the n-type samples; the likely cause is the stronger injection-level dependence of the lifetime, providing stricter limits for the parameters in the model.

D. Combined analysis of defect parameters of Cr_i and CrB pairs

Figure 10 shows the lifetime measurements for the p-type Cr-doped samples directly after quenching in water. In this state, the lifetime is decided by both the SRH lifetime of Cr_i and the SRH lifetime of CrB pairs: $1/\tau_{eff} = 1/\tau_{Cr_i} + 1/\tau_{CrB}$. We fit this set of lifetime data with linear combinations of Cr_i and CrB pairs, with the unpaired fraction as a fit parameter varied between 85% and 100% as described above, and allowing 11% relative error in lifetime data. Figure 11 shows the sum of squared residuals S as a function of both of the capture cross section ratios, with all other parameters fixed at their optimal values. The white regions depict the combinations of k^{Cr_i} and k^{CrB}, which generated unacceptable fitting. As shown in this colour map, fitting this set of lifetime data helps narrow down the ranges of k^{Cr_i} and k^{CrB}. Meanwhile, it also narrows down the ranges of the capture cross sections. The optimal values and ranges of the defect parameters found are shown in Table II, in comparison with the literature. As can be seen, the final values of the defect parameters are in a relatively tight range while in good agreement with previously determined data. These optimal values are used in SRH fits in Figures 2, 3, 5, 8, and 10. Note that a different choice of segregation coefficient for Cr would not change the energy levels or the capture cross section ratios determined in this work, but would lead to a

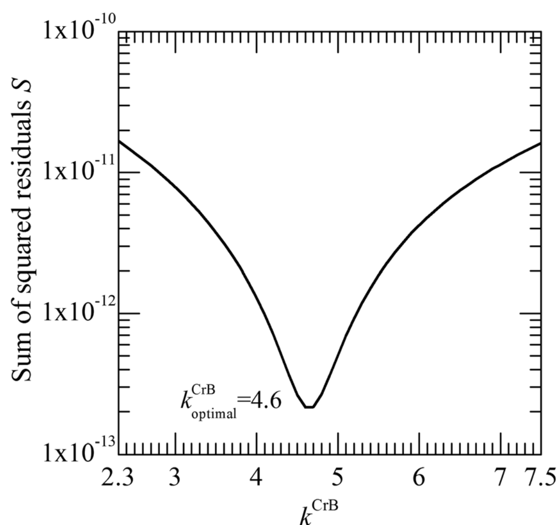

FIG. 9. The sum of squared residuals S as a function of k^{CrB}, obtained by fitting the lifetime data of p-type samples in the fully associated state, the optimal value being 4.6, with a range of (2.3, 7.5).

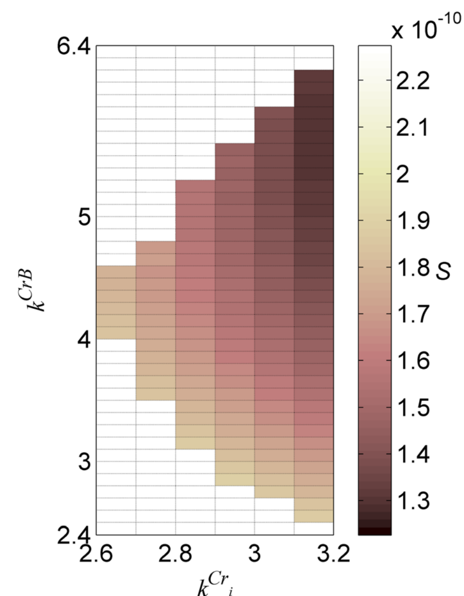

FIG. 11. The sum of squared residuals S as a function of k^{Cr_i} and k^{CrB}. Combinations in the white regions are found unfeasible. The fitted optimal values are $k^{Cr_i} = 3.2$ and $k^{CrB} = 5.8$.

[This article is copyrighted as indicated in the article. Reuse of AIP content is subject to the terms at: http://scitation.aip.org/termsconditions. Downloaded to] IP: 130.56.107.193 On: Mon, 15 Sep 2014 05:43:37

linear change in the capture cross sections. The reason for the linear dependence is that the exponent in Scheil's law, $k_{eff} - 1$, can be reduced to -1 when k_{eff} has a value orders of magnitude lower than 1.

Figure 12 compares the SRH lifetime of Cr_i and CrB pairs in p-Si with doping levels in the range of 1×10^{15}–$1 \times 10^{16}\,cm^{-3}$, predicted with the defect parameters found in this work (Table II). When $N_A = 2.8 \times 10^{15}\,cm^{-3}$, the lifetime of Cr_i is predicted to be injection- independent. The curves show a degradation of lifetime with higher doping levels. As predicted, CrB is always more recombination active than interstitial chromium up to the injection level around $\Delta n = 1 \times 10^{17}\,cm^{-3}$. However, Schmidt *et al.* predicted that Cr_i will become a stronger recombination center when the doping is higher than $N_A = 4 \times 10^{15}\,cm^{-3}$.[5] As shown in Figure 3, we observed a gradual degradation after annealing for all the p-type samples with $N_A = 1.11 \times 10^{16}$–$1.37 \times 10^{16}\,cm^{-3}$, showing that at least in this range of doping level, CrB is still the stronger recombination center. Our experimental results and modelling is in good agreement with the findings of Habenicht *et al.*, who experimentally confirmed that CrB is indeed always more recombination active within a range of N_A as large as 1–$4 \times 10^{16}\,cm^{-3}$.[14]

E. Comparison of Cr_i in n- and p-type silicon

Figure 13 compares the lifetime measurements for n- and p-type Cr-doped samples, with similar doping levels and concentrations of chromium. The estimated chromium concentrations are $[Cr] = 0.87 \times 10^{12}\,cm^{-3}$ and $[Cr] = 0.83 \times 10^{12}\,cm^{-3}$, respectively. For the p-type sample, the lifetime measured in the fully associated state as well as that measured directly after quenching are shown, and the modelled SRH lifetime in the fully dissociated state is also included. As shown by the curves, the n-type sample has a lifetime well above the p-type sample in any state.

Figure 14 models the SRH lifetime of Cr_i for both n-Si and p-Si with the same doping levels and concentration of chromium. The curves show a degradation of lifetime with higher doping levels. According to Eqs. (5) and (6), the high-injection SRH lifetime can be given by

$$\tau_{SRH,\,high-injection} = \frac{k+1}{N_t \sigma_n v_{th}}, \quad (9)$$

and is therefore, the same for both types for all the doping levels. It confirms our prediction that n-type silicon has higher lifetimes than p-Si at similar doping and chromium-contamination levels. Metals from Group 8 and below (Fe, Mo, Cr, V, Ti) tend to occupy interstitial sites in silicon at room temperature;[1,7] Macdonald and Geerligs showed that they are mostly donor-like and thus tend to have larger electron capture cross sections than hole capture cross sections ($k > 1$), which implies that they are generally more recombination active in p-Si than n-Si.[18] Our study experimentally demonstrates that this conclusion is also valid for chromium.

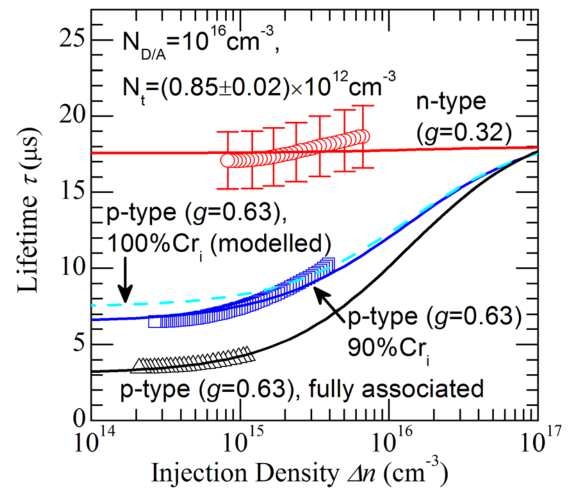

FIG. 13. Lifetime measurements (symbols) for samples n-type ($g = 0.32$) and p-type ($g = 0.63$). The data are fitted (solid line) with the defect parameters found in this work (Table II), which are also used to model the lifetime of p-type ($g = 0.32$) in the fully dissociated state.

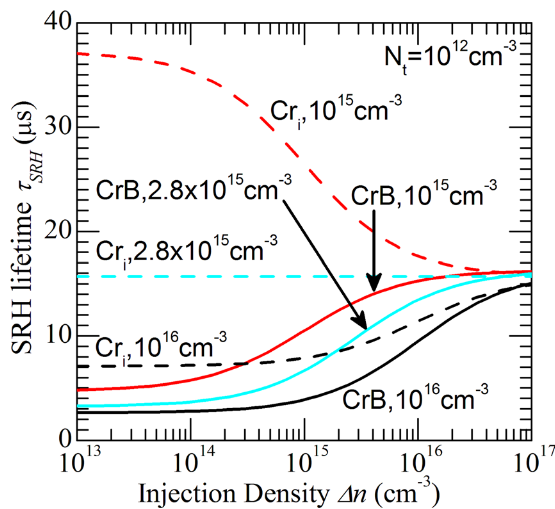

FIG. 12. Comparison of Cr_i and CrB SRH injection-dependent lifetime curves in p-type silicon with different doping levels. The curves are modeled with $N_t = 1 \times 10^{12}\,cm^{-3}$ and the defect parameters found in this work (Table II).

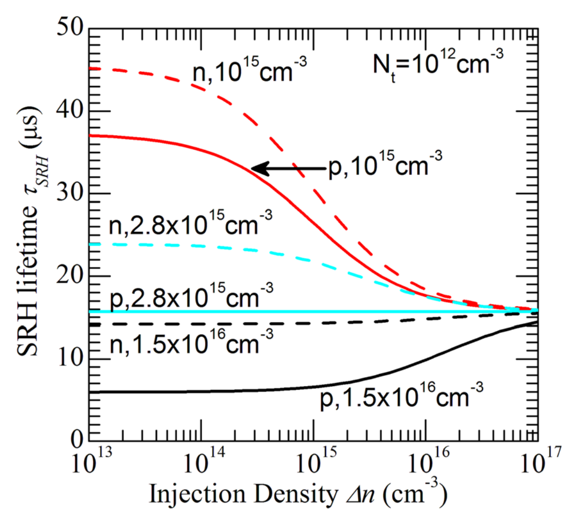

FIG. 14. Comparison of Cr_i SRH injection-dependent lifetime curves in p-type and n-type silicon with different doping levels. The curves are modelled with $N_t = 1 \times 10^{12}\,cm^{-3}$ and the defect parameters found in this work (Table II).

[This article is copyrighted as indicated in the article. Reuse of AIP content is subject to the terms at: http://scitation.aip.org/termsconditions. Downloaded to] IP: 130.56.107.193 On: Mon, 15 Sep 2014 05:43:37

Naturally, chromium exists as CrB pairs in p-Si under standard solar cell operation conditions. As we have demonstrated that in p-Si, CrB pairs are always more recombination active than Cr_i, we can conclude that chromium has a greater negative impact on carrier lifetimes in p-type silicon than n-type silicon with similar doping levels.

V. CONCLUSIONS

Defect parameters of Cr_i and CrB pairs have been determined by fitting doping level- and injection-dependent lifetimes measured on several n- and p-type samples. With a combined analysis of the two defects with the lifetime data measured on both n- and p-type samples, we are able to achieve relatively tight ranges of the defect recombination parameters. The capture cross section ratios of Cr_i and CrB determined in this work are 3.2 (-0.6, $+0$) and 5.8 (-3.4, $+0.6$), respectively. As shown by the experimental data as well as modelling, CrB pairs are always more recombination active than Cr_i in p-Si. In addition, both the experimental data and the modelling results show that Cr_i is generally more recombination active in p-Si than n-Si. Since dissolved chromium will always exist as CrB pairs in p-Si under standard solar cell operation conditions, we can conclude that Cr has a greater negative impact on carrier lifetimes in p-type silicon than n-type silicon with similar doping levels.

ACKNOWLEDGMENTS

This work has been supported through the Australian Renewable Energy Agency (ARENA) fellowships program, Project 1-GER010, and the Australian Centre for Advanced Photovoltaics; and also by the Australian Research Council (ARC) Future Fellowships program.

[1] K. Graff, *Metal Impurities in Silicon-Device Fabrication* (Springer Berlin, 2000).
[2] A. A. Istratov, T. Buonassisi, R. McDonald, A. Smith, R. Schindler, J. Rand, J. P. Kalejs, and E. R. Weber, J. Appl. Phys. **94**, 6552 (2003).
[3] D. Macdonald, A. Cuevas, A. Kinomura, Y. Nakano, and L. Geerligs, J. Appl. Phys. **97**, 033523 (2005).
[4] K. Mishra, Appl. Phys. Lett. **68**, 3281 (1996).
[5] J. Schmidt, R. Krain, K. Bothe, G. Pensl, and S. Beljakowa, J. Appl. Phys. **102**, 123701 (2007).
[6] L. Kimerling and J. Benton, Physica B+C **116**, 297 (1983).
[7] E. R. Weber, Appl. Phys. A **30**, 1 (1983).
[8] F. E. Rougieux, Ph.D. dissertation, Australian National University, 2012.
[9] G. Zoth and W. Bergholz, J. Appl. Phys. **67**, 6764 (1990).
[10] D. Macdonald, L. Geerligs, and A. Azzizi, J. Appl. Phys. **95**, 1021 (2004).
[11] S. Dubois, O. Palais, and P. Ribeyron, Appl. Phys. Lett. **89**, 232112 (2006).
[12] T. Trupke, R. Bardos, M. Schubert, and W. Warta, Appl. Phys. Lett. **89**, 044107 (2006).
[13] D. Macdonald, J. Tan, and T. Trupke, J. Appl. Phys. **103**, 073710 (2008).
[14] H. Habenicht, M. C. Schubert, and W. Warta, J. Appl. Phys. **108**, 034909 (2010).
[15] M. C. Schubert, H. Habernicht, and W. Warta, IEEE J. Photovoltaics **1**, 168 (2011).
[16] S. Lim, F. Rougieux, and D. Macdonald, Appl. Phys. Lett. **103**, 092105 (2013).
[17] H. Conzelmann, K. Graff, and E. Weber, Appl. Phys. A **30**, 169 (1983).
[18] D. Macdonald and L. Geerligs, Appl. Phys. Lett. **85**, 4061 (2004).
[19] D. Macdonald, Appl. Phys. A **81**, 1619 (2005).
[20] R. Sachdeva, A. Istratov, and E. Weber, Appl. Phys. Lett. **79**, 2937 (2001).
[21] S. Rein, *Lifetime Spectroscopy: A Method of Defect Characterization in Silicon for Photovoltaic Applications* (Springer, 2006), Vol. 85.
[22] J. Schmidt and A. Cuevas, J. Appl. Phys. **86**, 3175 (1999).
[23] D. Macdonald, A. Cuevas, and J. Wong-Leung, J. Appl. Phys. **89**, 7932 (2001).
[24] See http://www.siliconsultant.com/ for the information of Siliconsultant.
[25] E. Scheil, Zeitschrift für Metallkunde **34**, 70 (1942).
[26] R. A. Brown and D. H. Kim, J. Cryst. Growth **109**, 50 (1991).
[27] H. Kodera, Jpn. J. Appl. Phys., Part 1 **2**, 212 (1963).
[28] A. L. Blum, J. S. Swirhun, R. A. Sinton, F. Yan, S. Herasimenka, T. Roth, K. Lauer, J. Haunschild, B. Lim, K. Bothe, Z. Hameiri, B. Seipel, R. Xiong, M. Dhamrin, and J. D. Murphy, IEEE J. Photovoltaics **4**, 525 (2014).
[29] R. Hopkins, R. Seidensticker, J. Davis, P. Rai-Choudhury, P. Blais, and J. McCormick, J. Cryst. Growth **42**, 493 (1977).
[30] B. Bathey and M. Cretella, J. Mater. Sci. **17**, 3077 (1982).
[31] T. Lauinger, J. Schmidt, A. G. Aberle, and R. Hezel, Appl. Phys. Lett. **68**, 1232 (1996).
[32] J. Schmidt and A. G. Aberle, J. Appl. Phys. **81**, 6186 (1997).
[33] J. Schmidt and K. Bothe, Phys. Rev. B **69**, 024107 (2004).
[34] S. Park and D. Schroder, J. Appl. Phys. **78**, 801 (1995).
[35] H. Reiss, C. S. Fuller, and F. J. Morin, Bell Syst. Tech. J. **35**, 535 (1956).
[36] H. Nakashima, T. Sadoh, H. Kitagawa, and K. Hashimoto, Mater. Sci. Forum **143–147**, 761 (1994).
[37] R. A. Sinton and A. Cuevas, Appl. Phys. Lett. **69**, 2510 (1996).
[38] "A method to measure the lifetime of small-radius and arbitrary-shaped samples with QSSPC" (unpublished).
[39] K. Bothe and J. Schmidt, J. Appl. Phys. **99**, 013701 (2006).
[40] J. S. Blakemore, *Semiconductor Statistics, International Series of Monographs on Semiconductors* (Pergamon Press, Oxford, 1962), Vol. 3.
[41] D. Macdonald and A. Cuevas, Phys. Rev. B **67**, 075203 (2003).
[42] W. M. Bullis and H. R. Huff, J. Electrochem. Soc. **143**, 1399 (1996).
[43] A. Hangleiter, Phys. Rev. B **35**, 9149 (1987).

[This article is copyrighted as indicated in the article. Reuse of AIP content is subject to the terms at: http://scitation.aip.org/termsconditions. Downloaded to] IP: 130.56.107.193 On: Mon, 15 Sep 2014 05:43:37